

# Nuclear Effects on $R = \sigma_L/\sigma_T$ in Deep-Inelastic Scattering

*The HERMES Collaboration*

K. Ackerstaff<sup>5</sup>, A. Airapetian<sup>33</sup>, N. Akopov<sup>33</sup>, I. Akushevich<sup>6</sup>, M. Amarian<sup>25,28,33</sup>, E.C. Aschenauer<sup>6,13,25</sup>, H. Avakian<sup>10</sup>, R. Avakian<sup>33</sup>, A. Avetissian<sup>33</sup>, B. Bains<sup>15</sup>, C. Baumgarten<sup>23</sup>, M. Beckmann<sup>12</sup>, S. Belostotski<sup>26</sup>, J.E. Belz<sup>29,30</sup>, Th. Benisch<sup>8</sup>, S. Bernreuther<sup>8</sup>, N. Bianchi<sup>10</sup>, J. Blouw<sup>25</sup>, H. Böttcher<sup>6</sup>, A. Borissov<sup>5,14</sup>, M. Bouwuis<sup>15</sup>, J. Brack<sup>4</sup>, S. Brauksiepe<sup>12</sup>, B. Braun<sup>8,23</sup>, B. Bray<sup>3</sup>, St. Brons<sup>6</sup>, W. Brückner<sup>14</sup>, A. Brüll<sup>14</sup>, E.E.W. Bruins<sup>20</sup>, H.J. Bulten<sup>18,25,32</sup>, G.P. Capitani<sup>10</sup>, P. Carter<sup>3</sup>, P. Chumney<sup>24</sup>, E. Cisbani<sup>28</sup>, G.R. Court<sup>17</sup>, P. F. Dalpiaz<sup>9</sup>, E. De Sanctis<sup>10</sup>, D. De Schepper<sup>2,20</sup>, E. Devitsin<sup>22</sup>, P.K.A. de Witt Huberts<sup>25</sup>, P. Di Nezza<sup>10</sup>, M. Düren<sup>8</sup>, A. Dvoredsky<sup>3</sup>, G. Elbakian<sup>33</sup>, J. Ely<sup>4</sup>, A. Fantoni<sup>10</sup>, A. Fechtchenko<sup>7</sup>, M. Ferstl<sup>8</sup>, K. Fiedler<sup>8</sup>, B.W. Filippone<sup>3</sup>, H. Fischer<sup>12</sup>, B. Fox<sup>4</sup>, J. Franz<sup>12</sup>, S. Frullani<sup>28</sup>, M.-A. Funk<sup>5</sup>, Y. Gärber<sup>6</sup>, H. Gao<sup>2,15,20</sup>, F. Garibaldi<sup>28</sup>, G. Gavrilo<sup>26</sup>, P. Geiger<sup>14</sup>, V. Gharibyan<sup>33</sup>, A. Golendukhin<sup>5,19,23,33</sup>, G. Graw<sup>23</sup>, O. Grebeniuk<sup>26</sup>, P.W. Green<sup>1,30</sup>, L.G. Greeniaus<sup>1,30</sup>, C. Grosshauser<sup>8</sup>, M. Guidal<sup>25</sup>, A. Gute<sup>8</sup>, V. Gyurjyan<sup>10</sup>, J.P. Haas<sup>24</sup>, W. Haeberli<sup>18</sup>, J.-O. Hansen<sup>2</sup>, M. Hartig<sup>30</sup>, D. Hasch<sup>6,10</sup>, O. Häusser<sup>129,30</sup>, F.H. Heinsius<sup>12</sup>, R. Henderson<sup>30</sup>, M. Heno<sup>8</sup>, R. Hertenberger<sup>23</sup>, Y. Holler<sup>5</sup>, R.J. Holt<sup>15</sup>, W. Hoprich<sup>14</sup>, H. Ihssen<sup>5,25</sup>, M. Iodice<sup>28</sup>, A. Izotov<sup>26</sup>, H.E. Jackson<sup>2</sup>, A. Jgoun<sup>26</sup>, R. Kaiser<sup>6,29,30</sup>, E. Kinney<sup>4</sup>, M. Kirsch<sup>8</sup>, A. Kisselev<sup>26</sup>, P. Kitching<sup>1</sup>, H. Kobayashi<sup>31</sup>, N. Koch<sup>19</sup>, K. Königsmann<sup>12</sup>, M. Kolstein<sup>25</sup>, H. Kolster<sup>23</sup>, V. Korotkov<sup>6</sup>, W. Korsch<sup>3,16</sup>, V. Kozlov<sup>22</sup>, L.H. Kramer<sup>11,20</sup>, V.G. Krivokhijine<sup>7</sup>, M. Kurisuno<sup>31</sup>, G. Kyle<sup>24</sup>, W. Lachnit<sup>8</sup>, P. Lenisa<sup>9</sup>, W. Lorenzon<sup>21</sup>, N.C.R. Makins<sup>2,15</sup>, F.K. Martens<sup>1</sup>, J.W. Martin<sup>20</sup>, F. Masoli<sup>9</sup>, A. Mateos<sup>20</sup>, M. McAndrew<sup>17</sup>, K. McIlhenny<sup>3,20</sup>, R.D. McKeown<sup>3</sup>, F. Meissner<sup>6</sup>, F. Menden<sup>12,30</sup>, A. Metz<sup>23</sup>, N. Meyners<sup>5</sup>, O. Mikloukko<sup>26</sup>, C.A. Miller<sup>1,30</sup>, M.A. Miller<sup>15</sup>, R. Milner<sup>20</sup>, A. Most<sup>15,21</sup>, V. Muccifora<sup>10</sup>, R. Mussa<sup>9</sup>, A. Nagaitsev<sup>7</sup>, Yu. Naryshkin<sup>26</sup>, A.M. Nathan<sup>15</sup>, F. Neunreither<sup>8</sup>, J.M. Niczyporuk<sup>15,20</sup>, W.-D. Nowak<sup>6</sup>, M. Nupieri<sup>10</sup>, T.G. O'Neill<sup>2</sup>, R. Openshaw<sup>30</sup>, J. Ouyang<sup>30</sup>, B.R. Owen<sup>15</sup>, V. Papavassiliou<sup>24</sup>, S.F. Pate<sup>20,24</sup>, M. Pitt<sup>3</sup>, S. Potashov<sup>22</sup>, D.H. Potterveld<sup>2</sup>, G. Rakness<sup>4</sup>, A. Reali<sup>9</sup>, R. Redwine<sup>20</sup>, A.R. Reolon<sup>10</sup>, R. Ristinen<sup>4</sup>, K. Rith<sup>8</sup>, P. Rossi<sup>10</sup>, S. Rudnitsky<sup>21</sup>, M. Ruh<sup>12</sup>, D. Ryckbosch<sup>13</sup>, Y. Sakemi<sup>31</sup>, I. Savin<sup>7</sup>, C. Scarlett<sup>21</sup>, A. Schäfer<sup>27</sup>, F. Schmidt<sup>8</sup>, H. Schmitt<sup>12</sup>, G. Schnell<sup>24</sup>, K.P. Schüller<sup>5</sup>, A. Schwind<sup>6</sup>, J. Seibert<sup>12</sup>, T.-A. Shibata<sup>31</sup>, K. Shibatani<sup>31</sup>, T. Shin<sup>20</sup>, V. Shutov<sup>7</sup>, C. Simani<sup>9</sup>, A. Simon<sup>12,24</sup>, K. Sinram<sup>5</sup>, P. Slavich<sup>9,10</sup>, M. Spengos<sup>5</sup>, E. Steffens<sup>8</sup>, J. Stenger<sup>8</sup>, J. Stewart<sup>17</sup>, U. Stoesslein<sup>6</sup>, M. Sutter<sup>20</sup>, H. Tallini<sup>17</sup>, S. Taroian<sup>33</sup>, A. Terkulov<sup>22</sup>, E. Thomas<sup>10</sup>, B. Tipton<sup>20</sup>, M. Tytgat<sup>13</sup>, G.M. Urciuoli<sup>28</sup>, J.F.J. van den Brand<sup>25,32</sup>, G. van der Steenhoven<sup>25</sup>, R. van de Vyver<sup>13</sup>, J.J. van Hunen<sup>25</sup>, M.C. Vetterli<sup>29,30</sup>, V. Vikhrov<sup>26</sup>, M.G. Vincter<sup>1,30</sup>, J. Visser<sup>25</sup>, E. Volk<sup>14</sup>, W. Wander<sup>8,20</sup>, J. Wendland<sup>29</sup>, S.E. Williamson<sup>15</sup>, T. Wise<sup>18</sup>, K. Woller<sup>5</sup>, S. Yoneyama<sup>31</sup>, H. Zohrabian<sup>33</sup>,

<sup>1</sup>Department of Physics, University of Alberta, Edmonton, Alberta T6G 2J1, Canada

<sup>2</sup>Physics Division, Argonne National Laboratory, Argonne, Illinois 60439-4843, USA

<sup>3</sup>W.K. Kellogg Radiation Laboratory, California Institute of Technology, Pasadena, California 91125, USA

<sup>4</sup>Nuclear Physics Laboratory, University of Colorado, Boulder, Colorado 80309-0446, USA

<sup>5</sup>DESY, Deutsches Elektronen Synchrotron, 22603 Hamburg, Germany

<sup>6</sup>DESY Zeuthen, 15738 Zeuthen, Germany

<sup>7</sup>Joint Institute for Nuclear Research, 141980 Dubna, Russia

<sup>8</sup>Physikalisches Institut, Universität Erlangen-Nürnberg, 91058 Erlangen, Germany

<sup>9</sup>Istituto Nazionale di Fisica Nucleare, Sezione di Ferrara and Dipartimento di Fisica, Università di Ferrara, 44100 Ferrara, Italy

<sup>10</sup>Istituto Nazionale di Fisica Nucleare, Laboratori Nazionali di Frascati, 00044 Frascati, Italy

<sup>11</sup>Department of Physics, Florida International University, Miami, Florida 33199, USA

<sup>12</sup>Fakultät für Physik, Universität Freiburg, 79104 Freiburg, Germany

<sup>13</sup>Department of Subatomic and Radiation Physics, University of Gent, 9000 Gent, Belgium

<sup>14</sup>Max-Planck-Institut für Kernphysik, 69029 Heidelberg, Germany

<sup>15</sup>Department of Physics, University of Illinois, Urbana, Illinois 61801, USA

<sup>16</sup>Department of Physics and Astronomy, University of Kentucky, Lexington, Kentucky 40506, USA

<sup>17</sup>Physics Department, University of Liverpool, Liverpool L69 7ZE, United Kingdom

<sup>18</sup>Department of Physics, University of Wisconsin-Madison, Madison, Wisconsin 53706, USA

<sup>19</sup>Physikalisches Institut, Philipps-Universität Marburg, 35037 Marburg, Germany

<sup>20</sup>Laboratory for Nuclear Science, Massachusetts Institute of Technology, Cambridge, Massachusetts 02139, USA

<sup>21</sup>Randall Laboratory of Physics, University of Michigan, Ann Arbor, Michigan 48109-1120, USA

<sup>22</sup>Lebedev Physical Institute, 117924 Moscow, Russia

<sup>23</sup>Sektion Physik, Universität München, 85748 Garching, Germany

<sup>24</sup>Department of Physics, New Mexico State University, Las Cruces, New Mexico 88003, USA

<sup>25</sup>Nationaal Instituut voor Kernfysica en Hoge-Energiefysica (NIKHEF), 1009 DB Amsterdam, The Netherlands

<sup>26</sup> Petersburg Nuclear Physics Institute, St. Petersburg, 188350 Russia

<sup>27</sup> Institut für Theoretische Physik, Universität Regensburg, 93040 Regensburg, Germany

<sup>28</sup> Istituto Nazionale di Fisica Nucleare, Sezione Sanità and Physics Laboratory, Istituto Superiore di Sanità, 00161 Roma, Italy

<sup>29</sup> Department of Physics, Simon Fraser University, Burnaby, British Columbia V5A 1S6, Canada

<sup>30</sup> TRIUMF, Vancouver, British Columbia V6T 2A3, Canada

<sup>31</sup> Department of Physics, Tokyo Institute of Technology, Tokyo 152, Japan

<sup>32</sup> Department of Physics and Astronomy, Vrije Universiteit, 1081 HV Amsterdam, The Netherlands

<sup>33</sup> Yerevan Physics Institute, 375036, Yerevan, Armenia

(October 18, 1999)

Cross section ratios for deep-inelastic scattering from  $^{14}\text{N}$  and  $^3\text{He}$  with respect to  $^2\text{H}$  have been measured by the HERMES experiment at DESY using a 27.5 GeV positron beam. The data cover a range in the Bjorken scaling variable  $x$  between 0.013 and 0.65, while the negative squared four-momentum transfer  $Q^2$  varies from 0.5 to 15 GeV<sup>2</sup>. The data are compared to measurements performed by NMC, E665, and SLAC on  $^4\text{He}$  and  $^{12}\text{C}$ , and are found to be different for  $x < 0.06$  and  $Q^2 < 1.5$  GeV<sup>2</sup>. The observed difference is attributed to an  $A$ -dependence of the ratio  $R = \sigma_L/\sigma_T$  of longitudinal to transverse deep-inelastic scattering cross sections at low  $x$  and low  $Q^2$ .

PACS numbers: 13.60.Hb, 13.60.-r, 24.85.+p, 12.38.-t

The energy scales relevant to deep-inelastic lepton nucleon scattering (multi-GeV) greatly differ from those relevant to the atomic nucleus (multi-MeV). Hence, it came as a surprise that the structure function  $F_2^N(x)$ , which in the Quark-Parton Model represents the quark momentum distribution inside the nucleon, was found to depend on the mass  $A$  of the atomic nucleus [1]. This phenomenon is known as the *EMC effect* at large values of the Bjorken scaling variable  $x$ , i.e.  $x > 0.1$ , and as *shadowing* at lower values of  $x$  [2].

With  $F_2(x)$  found to be  $A$ -dependent, it is relevant to investigate whether this dependence is the same for its longitudinal and transverse components,  $F_L(x)$  and  $F_1(x)$ . The latter two structure functions are related to  $F_2(x)$  via  $F_L(x) = (1 + Q^2/\nu^2)F_2(x) - 2xF_1(x)$  with  $Q^2$  the negative of the four-momentum transfer squared  $q^2$ ,  $\nu$  the energy transfer,  $x = Q^2/2M\nu$  and  $M$  the nucleon mass. A possible difference of the  $A$ -dependence of  $F_L(x)$  and  $F_1(x)$  can be investigated by measuring the ratio of longitudinal to transverse deep-inelastic scattering (DIS) cross sections  $R = \sigma_L/\sigma_T = F_L(x)/2xF_1(x)$  for various nuclear targets.

Theoretically, a possible  $A$ -dependence of  $R$  has been suggested by several authors. In ref. [3] the Fermi motion of the nucleons is seen to enhance higher-twist effects, which will lead to an enhancement of  $F_L(x)$  at low values of  $x$  and  $Q^2$ . It has also been argued [4] that an increase of the nuclear gluon distribution may lead to an enhancement of  $R$ . On the other hand, in ref. [5] it is suggested that nuclear shadowing might be different for the longitudinal and transverse DIS cross sections. The predicted size and  $(x, Q^2)$ -dependence of these effects are all different. However, no experimental evidence for an  $A$ -dependence of  $R$  has been found to date [6–9].

In this Letter we present data from the HERMES experiment on the cross section ratio for deep-inelastic positron scattering off nitrogen and helium-3 with respect to deuterium. These ratios are compared to similar ratios measured in deep-inelastic scattering by NMC [10], E665 [11], and SLAC [12]. The ratio of the inclusive DIS cross sections on  $^{14}\text{N}$  ( $^3\text{He}$ ) and  $^2\text{H}$  is presented in figure 1. A significant difference between the present data and previous data is observed for  $x < 0.06$ . In this domain the HERMES data for both nuclei are smaller than the NMC and E665 data and the deviation increases towards smaller values of  $x$ . At high values of  $x$  the HERMES data are in agreement with the SLAC data. In the following it is shown how the difference between the NMC and HERMES measurements can be attributed to an  $A$ -dependence of  $R$  at low values of  $x$  and  $Q^2$ .

Apart from the data shown in figure 1, other data exist which show a strong reduction of  $\sigma_A/\sigma_D$  for  $0.01 < x < 0.1$  and  $0.05 < Q^2 < 1.5 \text{ GeV}^2$  that is similar to that of the HERMES data on  $^{14}\text{N}$  [13,14]. However, these data were never used to study a possible  $A$ -dependence of  $R$ , either because of insufficient statistics [14], or because of

their limited kinematic coverage [13].

In deep-inelastic charged lepton scattering from an unpolarised target, the double-differential cross section per nucleon can be written in the one-photon exchange approximation as

$$\begin{aligned} \frac{d^2\sigma}{dx dQ^2} &= \frac{4\pi\alpha^2}{Q^4} \frac{F_2(x, Q^2)}{x} \times \\ &\left[ 1 - y - \frac{xyM}{2E} + \frac{y^2}{2} \left( \frac{1 + 4M^2x^2/Q^2}{1 + R(x, Q^2)} \right) \right] \\ &= \frac{\sigma_{\text{Mott}}}{E'E} \frac{\pi F_2(x, Q^2)}{x\epsilon} \left[ \frac{1 + \epsilon R(x, Q^2)}{1 + R(x, Q^2)} \right], \end{aligned} \quad (1)$$

where  $y = \nu/E$ ,  $\sigma_{\text{Mott}}$  represents the cross section for lepton scattering from a point charge, and  $E$  and  $E'$  are the initial and final lepton energy, respectively. The virtual photon polarisation parameter is given by

$$\epsilon = \frac{4(1-y) - \frac{Q^2}{E^2}}{4(1-y) + 2y^2 + \frac{Q^2}{E^2}}. \quad (2)$$

The ratio of DIS cross sections from nucleus  $A$  and deuterium  $D$  ( $=^2\text{H}$ ) is then given by:

$$\frac{\sigma_A}{\sigma_D} = \frac{F_2^A}{F_2^D} \frac{(1 + \epsilon R_A)(1 + R_D)}{(1 + R_A)(1 + \epsilon R_D)}, \quad (3)$$

where  $R_A$  and  $R_D$  represent the ratio  $\sigma_L/\sigma_T$  for nucleus  $A$  and deuterium. For  $\epsilon \rightarrow 1$  the cross section ratio equals the ratio of structure functions  $F_2^A/F_2^D$ . For smaller values of  $\epsilon$  the cross section ratio is equal to  $F_2^A/F_2^D$  only if  $R_A = R_D$ . A difference between  $R_A$  and  $R_D$  will thus introduce an  $\epsilon$ -dependence of  $\sigma_A/\sigma_D$ . Hence, measurements of  $\sigma_A/\sigma_D$  as a function of  $\epsilon$  can be used to extract experimental information on  $R_A/R_D$ , if  $R_D$  is known.

The data presented in this paper were collected by the HERMES experiment at DESY using  $^1\text{H}$ ,  $^2\text{H}$ ,  $^3\text{He}$ , and  $^{14}\text{N}$  internal gas targets in the 27.5 GeV positron storage ring of HERA. The target gases were injected into a tubular open-ended storage cell inside the positron ring. The cell provides a 40 cm long target with areal densities of up to  $6 \times 10^{15}$  nucleons/cm $^2$  for  $^{14}\text{N}$ . The luminosity was measured by detecting Bhabha-scattered target electrons in coincidence with the scattered positrons, in a pair of NaBi(WO $_4$ ) $_2$  electromagnetic calorimeters. Dead times of less than 5% were observed even at the highest luminosities of about  $10^{33}$  nucleons/(cm $^2$ s). Systematic uncertainties in the measurements of the cross section ratios were minimized by cycling among different target gases every 2 – 4 hours during part of the data taking.

In the HERMES spectrometer [15] both the scattered positrons and the produced hadrons can be detected and identified within an angular acceptance  $\pm 170$  mrad horizontally, and 40 – 140 mrad vertically. The trigger was formed from a coincidence between a pair of scintillator

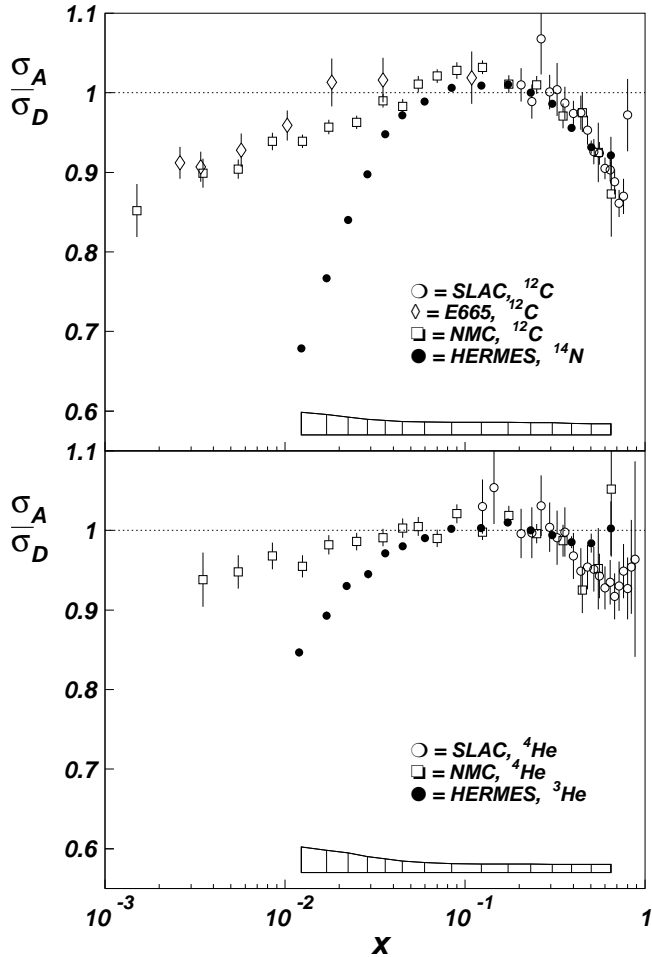


FIG. 1. Ratio of cross sections of inclusive deep-inelastic lepton scattering from nucleus  $A$  and  $D$  versus  $x$ . The error bars of the HERMES measurement represent the statistical uncertainties, the systematic uncertainty of the HERMES data is given by the error band. The error bars of the NMC, E665, and SLAC data are given by the quadratic sum of the statistical and systematic uncertainties.

hodoscope planes and a lead-glass calorimeter. The trigger required an energy of more than 3.5 GeV deposited in the calorimeter, resulting in a typical trigger rate of 100 Hz. Positron identification was accomplished using the calorimeter, the second hodoscope, which functioned as a preshower counter, a transition radiation detector, and a threshold gas Čerenkov counter. This system provided positron identification with an average efficiency of 99 % and a hadron contamination of less than 1 %.

Deep-inelastic scattering events were extracted from the data by imposing constraints on  $Q^2$ ,  $W$  (the invariant mass of the photon-nucleon system), and  $y$ . For each event it was required that  $Q^2 > 0.3 \text{ GeV}^2$ ,  $W > 2 \text{ GeV}$  and  $y < 0.85$ .

As the ratio  $\sigma_A/\sigma_D$  involves nuclei with different numbers of protons, radiative corrections do not cancel in the ratio. In particular, the radiative processes associated with elastic and quasi-elastic scattering are different for

the two target nuclei. These radiative corrections have been computed using the methods outlined in Ref. [16]. In the cross section ratio the correction associated with elastic (i.e. coherent) scattering from the target nucleus is dominant.

Several input parameters are needed for the calculation of the radiative corrections. For the evaluation of the coherent radiative tails, the nuclear elastic form factors must be known. Parameterisations of the form factors of  $^2\text{H}$ ,  $^3\text{He}$ , and  $^{14}\text{N}$  were taken from the literature [17–19]. For the quasi-elastic tails, the nucleon form factor parameterisation of Gari and Krümpelmann [20] was used. The reduction of the bound nucleon cross section with respect to the free nucleon one (quasi-elastic suppression) was evaluated using the results of a calculation by Bernabeu [21] for deuterium and the non-relativistic Fermi gas model for  $^3\text{He}$  and  $^{14}\text{N}$  [22]. The evaluation of the inelastic higher order QED processes requires the knowledge of both  $F_2$  and  $R$  over a wide range of  $x$  and  $Q^2$ . The structure function  $F_2^D(x, Q^2)$  was described by a parameterisation of the NMC, SLAC, and BCDMS data [23]; for  $R_D$  the Whitlow parameterisation [24] was used. As the values of  $F_2^A(x, Q^2)$  and  $R_A(x, Q^2)$  are unknown for  $^3\text{He}$  and  $^{14}\text{N}$ , an iterative procedure has been used. As a starting point the nuclear structure functions  $F_2^A(x, Q^2)$  were taken from phenomenological fits to the SLAC and NMC data, and  $R_A(x, Q^2)$  was assumed to be equal to  $R_D(x, Q^2)$ . The resulting radiatively corrected values of  $\sigma_A/\sigma_D$  were used to determine  $F_2^A/F_2^D$  and  $R_A/R_D$ , which were given as input to the radiative correction code in the next step until convergence was reached. It is noted that the large difference between the NMC/E665 and HERMES values of  $\sigma_A/\sigma_D$  is already present if the NMC and SLAC parameterisations are used for  $F_2(x, Q^2)$  and  $R(x, Q^2)$ . The iteration procedure, which converges in three steps, enlarges the difference by about 40 % (for  $^{14}\text{N}$ ) in the lowest  $x$  bins.

The size of the radiative corrections is largest in the lowest  $x$ -bin, where it amounts to 0.552, 0.461, and 0.372 for  $^2\text{H}$ ,  $^3\text{He}$ , and  $^{14}\text{N}$ , respectively. The systematic uncertainty in the radiative corrections was estimated by using upper and lower limits of the parameterisations, or alternative parameterisations [23–26] for all the above input parameters. The total systematic uncertainty in the cross section ratios varies from 5 % (4 %) at low  $x$  to 2 % (1 %) at high  $x$  for  $^{14}\text{N}$  ( $^3\text{He}$ ). It includes the normalization uncertainty of 2 % (1 %) and the uncertainty in the radiative corrections, which is dominant.

The effects originating from the finite resolution of the spectrometer and from the hadron contamination in the positron sample have been determined and found to be negligible. As a cross check of the understanding of the entire analysis chain including the radiative corrections, the cross section ratio of deuterium and hydrogen has been determined as a function of  $x$  and  $Q^2$ . The